Advances in Aerospace Science and Technology, 2016, 1, 48-57
Published Online June 2016 in SciRes. http://www.scirp.org/journal/aast
http://dx.doi.org/10.4236/aast.2016.11005

PTVC-M for Ultra-Agile VTOL and 300+ km·h^{-1} Cruising

Chung-Kiak Poh*, Chung-How Poh

Aero-Persistence Research, Penang, Malaysia
Email: *kiak@aero-persistence.com

Received 20 May 2016; accepted 28 May 2016; published 27 June 2016

Abstract

There remains a need to develop improved VTOL techniques that are cost-effective and with minimum compromise on cruising flight performance for fixed-wing aircraft. This work proposes an elegant VTOL control method known as PTVC-M (pitch-axis thrust vector control with moment arms) for tailsitters. The hallmark of the approach is the complete elimination of control surfaces such as elevators and rudder. Computer simulations with a 1580 mm wing span airplane reveal that the proposed technique results in authoritative control and unique maneuverability such as inverted vertical hover and stall-spin with positive climb rate. Zero-surface requirement of the PTVC-M virtually eliminates performance tradeoffs between VTOL and high-speed flight. In this proof-of-concept study, the VTOL-capable aircraft achieves a V_H of 360 km·h^{-1} at near sea-level. The proposed technique will benefit a broad range of applications including high-performance spinsonde that can directly measure 10-m surface wind, tropical cyclone research, and possibly serving as the cornerstone for the next-generation sport aerobatics.

Keywords

Pitch-Axis Thrust Vector Control, VTOL, Tailsitter, Ultra-Maneuverability

1. Introduction

In the early 1920s, Juan de la Cierva came up with the concept of autorotation in the efforts to solve the wing-stall problems [1]. His work and dedication to the development of autogyro have brought the notions of rotary wings and STOL (short takeoff and landing) to the aviation world [2]-[4]. Helicopters eventually emerged and since 1950s there have been quests for an aircraft that has the cruising efficiency of an airplane and the vertical takeoff and landing (VTOL) capability of a helicopter [5]. The Fairey Rotodyne has tip jet-powered rotor and

*Corresponding author.

How to cite this paper: Poh, C.-K. and Poh, C.-H. (2016) PTVC-M for Ultra-Agile VTOL and 300+ km·h^{-1} Cruising. *Advances in Aerospace Science and Technology*, **1**, 48-57. http://dx.doi.org/10.4236/aast.2016.11005

two turboprops mounted under its fixed-wings [6]. The jet-powered rotor was driven for vertical takeoffs, landings and hovering, but autorotation mode was used during cruising with the forward thrusts coming from the turboprops [6]. It held a world speed record of 307.2 $km \cdot h^{-1}$ but the program was unfortunately terminated in 1962 [6]. Throughout the years numerous VTOL-capable airplanes have emerged and among them were the Convair XFY Pogo, the Bell XV-3, the Yakovlev Yak-141, and the Bell XV-15 [5] [7]. Despite significant efforts on the development of VTOL airplanes, numerous challenges remain. The primary challenges are often associated with the mechanical complexities, cost-of-ownership and maintenance [5] [8]. The ability to overcome these challenges will promote the widespread use of VTOL airplanes especially for civilian applications. Autonomous applications such as weather surveillance in remote oceans for an extended period of time would require a reliable airframe to help ensure high rate of mission success [9]. VTOL-capable airplanes can be broadly divided into several classes, namely tiltrotor, tiltwing, and tailsitter [5]. More recent developments include stop-rotors and hybrid [10]-[14]. In our opinion, apart from cost and reliability considerations, an important attribute that will significantly enhance the usefulness of a VTOL airplane is ultra-maneuverability, especially in the domain of unmanned aircraft.

Modern aerobatic model airplanes have the abilities to perform an array of impressive post-stall maneuvers known as "3D aerobatics" such as hovering (including VTOL), waterfall, flatspin, blender, tailslide and their derivatives [15]-[17]. The flight performance, and design reliability of these airplanes have been put to test globally during weekend flying in aeromodelling clubs and in international competitions such as the prestigious Fédération Aéronautique Internationale (FAI) Class F3M [17]. The distinctive characteristics of these aircraft are their relatively large control surfaces immersed in strong propeller wash and thrust-to-weight ratio that exceeds unity [15]. These techniques can potentially be used to create VTOL airplanes with ultra-agility. However, two major setbacks of this approach are that the control surfaces have to be relatively large, and that they should be immersed in propeller wash, and these limit the application scope. For example, if the technique were to be applied to an aircraft with anhedral (reversed dihedral) horizontal stabilizers with wing-mounted propellers, the pitch control authority has been found to be asymmetrical depending on whether the aircraft is performing the upright "harrier" (*i.e.* to fly in trim with nose angle of 45˚ or greater) or the inverted "harrier". Similarly, considerations have to be given to the placement of the rudder. The challenge is less pronounced when it comes to roll control as the aileron (s) can be suitably located almost anywhere along the trailing edge of each wing. Additionally, large control surfaces often pose a performance tradeoff during high speed cruising due to flutter [18]. Thrust vector control (TVC) methods have been used on aircraft, rockets, and multirotor UAVs (unmanned aerial vehicles) to control altitude or angular velocity [19] [20].

To address the issues above in regard to the constraints imposed by the placement of rudder and elevators, this work proposes the concept of pitch-axis thrust vector control with moment arms (PTVC-M) in an attempt to create an ultra-agile 3-axis VTOL control method for tailsitters. The proposed PTVC-M requires no control surfaces to actuate VTOL flight controls so as to gain independence from the aerodynamic rudder and elevators. For an aircraft with twin-engine configuration (*i.e.*, one engine on each wing), the system will involve two pairs of moment arms; one of which is parallel with the longitudinal axis to enable pitch control and the other pair is parallel with the lateral axis to ensure responsive yaw. The flight performance is investigated via computer simulation using a 1580 mm wing span UAV as a test platform. In this article, the definition of a tailsitter is one whereby the roll axis (longitudinal axis) of the aircraft is approximately parallel with the z-axis of the world frame during the VTOL phase though the landing gears can be attached to any part of the airframe including fuselage and wing and are not restricted to the vertical or horizontal stabilizers at the rear of the aircraft.

2. Materials and Methods

2.1. Working Principle

In principle, the PTVC-M actuates pitch control by creating moments about the lateral axis (pitch axis) similar to conventional elevator effect, except the force is generated directly by the thrust-producing element instead of surface-derived aerodynamic force. In the case of propeller being the thrust-producing element, the moment arms extend from the center of the propeller disks to the lateral axis. In **Figure 1**, the pitching moment arm, L_1 is indicated for one set of wing. The yaw control of the PTVC-M is derived from the differential thrust of the propellers and a pair of moment arms. The yawing moment arm, L_2 is the distance from the center of the propeller disk to the centerline of the aircraft (**Figure 1**).

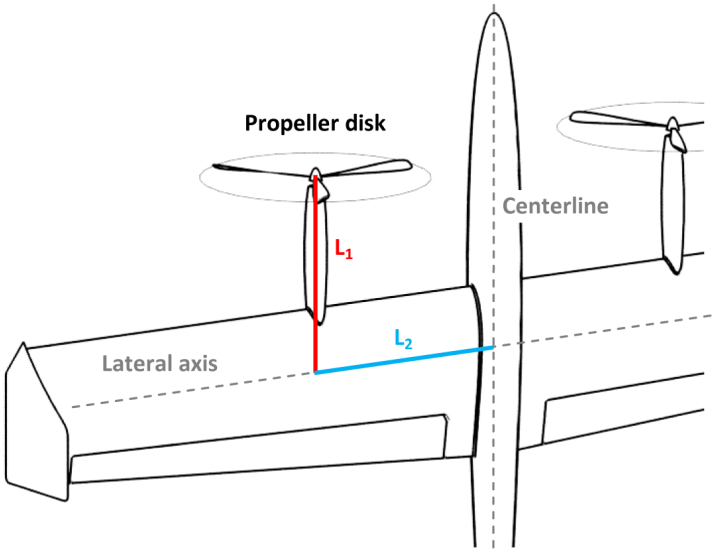

Figure 1. PTVC-M: illustration of the moment arms on one set of wing.

Therefore, the further away the location of the propeller from the centerline, the greater the maximum yaw moment. However, if the design intent requires the elevators to be partially immersed in the propeller wash to harness its additional advantages, then there should be an optimal placement of the propeller along the lateral axis because if placed too far out then there would be very little amount of propeller wash reaching the elevators at the rear of the fuselage. Apart from propeller, the thrust-producing element can include turbine fans, rotor blades, or possibly even rockets. The thrust-vectoring mechanism responsible for the tilting of the propeller disk can be realized using several well established methods such as swashplate or servo-actuated motor mounts similar to those being used for yaw control in present day tricopters [21] [22]. In the presence of downstream surfaces such as wing, the propeller wash effects [23] have to be considered. A way to avoid the propeller wash effect is to mount the thrust-producing elements towards the rear of the aircraft. However, such configuration may entail a more complex structural design. In this work, we will focus on a configuration in which the thrust-producing elements are mounted on the wing for the following reasons: 1) in the real-world scenario the wing spar would readily provide strong mounting points for the engine nacelle hence simplifying the structural design, and 2) control surfaces immersed in propeller wash will provide additional control authority and might allow a seamless transition in controls between VTOL and level flight.

2.2. Aircraft Design and Simulation Details

The graphical model of the small UAV used in this work was created using the Autodesk 3ds Max® [24]. The orientations of the pivots and naming convention of the components were as per the requirements and it was imported into the RealFlight®[1] 6.5 simulator [25] using the KEmax plugin [26]. Refinement of the computer model was done using the Accu-Model™ aircraft editor within the simulation software. The model UAV has a wing span of 1580 mm and a total body length of 1120 mm. The MH 22 airfoil [27] was used on the main wing to help achieve a high V_H (*i.e.* maximum speed in level flight with maximum continuous power). The model has twin motor, one on each side of the wing as shown in **Figure 2**. The airframe adopted the 3-piece stabilizers design, which consisted of a vertical stabilizer and two anhedral (reversed dihedral) horizontal stabilizers, spaced 120˚ apart from each other and they also functioned as part of the landing gears. Such configuration was expected to be lighter and has lower aerodynamic drags than the 4-piece stabilizers design commonly employed by tailsitters. The innovative "zero-surface" requirement of the proposed VTOL control technique enabled the designs of the aerodynamic rudder and elevator to be optimized for other phases of flight more critical to the primary roles of the aircraft such as high-speed cruising.

The surface areas of the rudder and elevators were approximately 32% of those of the stabilizers, which were significantly smaller than those on the "3D aerobatic" model aircraft [15] [16]. Maximum deflections of all the

[1]RealFlight is a registered trademark of Hobbico, Inc. used with permission.

Figure 2. Computer model of the twin-motor tailsitter incorporating the PTVC-M feature. The wing span is 1580 mm.

control surfaces were ±45˚. Optional retractable undercarriage can be affixed to the UAV to enable takeoff and landing on runway. The aircraft was equipped with two 3-bladed propellers and they were counter-rotating to each other. The variable pitch propeller has a diameter of 305 mm. Each brushless motor has a maximum electrical power of 4 kW. The all-up weight (AUW) of the aircraft was 2.48 kg with a wing loading of 60.3 gdm^{-2}. Gyros (electronic flight stabilization system) were added to the roll, pitch and yaw controls for the piloted simulations in this study. However, flight stabilization for a particular principal axis would be disengaged when performing the angular rate test so as to avoid any possible influence from the gyro. **Figure 3(a)** to **Figure 3(d)** show the angular displacements of the propellers with the control inputs. To better illustrate the tilting of the propellers in relation to the control inputs, the displacements of the propellers were coupled to the control surfaces. The following describes the flight control methodology of the aircraft:

Pitch: tilting both the propellers in the same direction [**Figure 3(a)**].

Roll: tilting the propellers by the same angular displacement but in opposite direction [**Figure 3(b)**].

Yaw: differential thrust by varying the rotational speed of the propellers [**Figure 3(c)**]. In this case, right rudder was applied and the left-hand side propeller was spinning while the right-hand side propeller was stationary. The throttle was at its lowest position.

Figure 3(d) depicts the tilting orientations of the propellers (neglecting the propeller wash effects on the roll control) when up-elevator and right-aileron were applied simultaneously.

3. Simulation Results and Discussion

3.1. Steady Level Flight Performance

The PTVC-M was deactivated and only the control surfaces were used during level flight evaluation, and the roll, pitch and yaw controls were found to be responsive. As shown in **Figure 4**, the maximum speed in level flight with maximum continuous power (V_H) was 360 ± 1 $km \cdot h^{-1}$ with total electrical power consumption of 6961 ± 1 W and the variometer indicated a vertical climb rate of 0 ms^{-1}. The power value displayed on the NavGuides in the upper left corner is the power consumption per motor. The stall speed (V_s) of the aircraft was determined to be 39 ± 1 $km \cdot h^{-1}$. Any maneuvers performed at airspeeds below the V_s are termed as post-stall maneuvers in this work. When power to the left motor was cut off at cruising speed of 250 $km \cdot h^{-1}$, the UAV yawed left and rolled left at rates of 14˚s^{-1} and 2˚s^{-1}, respectively which were well within the capacity of the rudder and ailerons to counteract. As mentioned above, the gyros for these controls were switched off during the test.

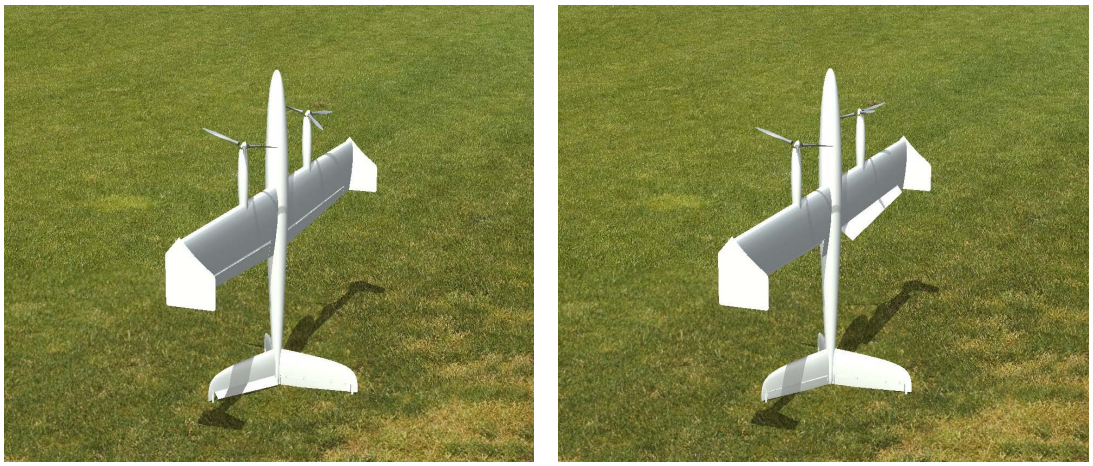

(a) Pitch (b) Roll

(c) Yaw (d) Simultaneous pitch and roll

Figure 3. Tilting orientations of the propellers with respect to the control inputs. Differential thrust was used to actuate yaw.

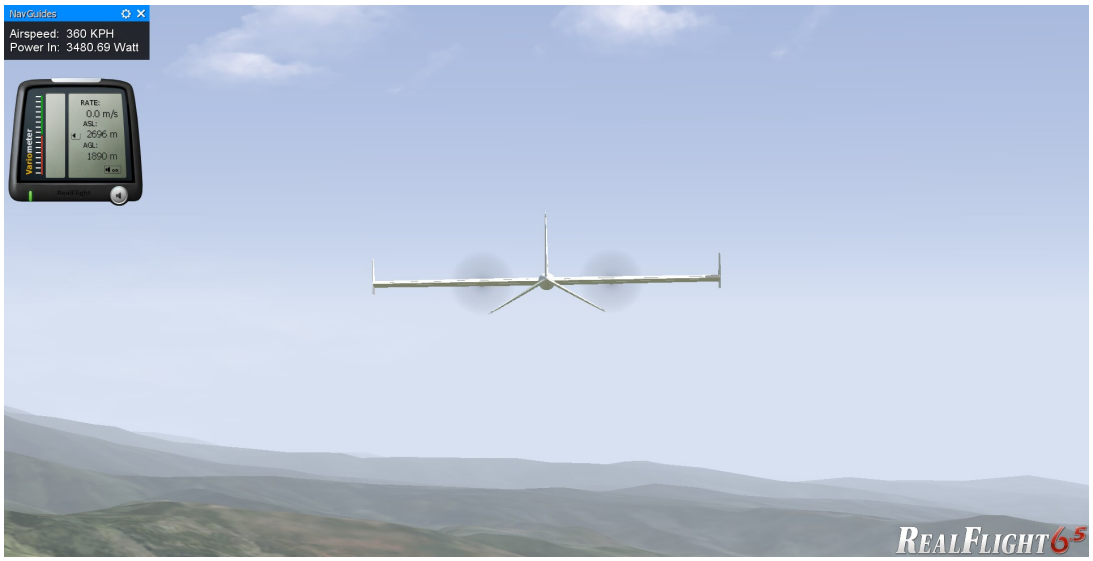

Figure 4. The tailsitter achieved a V_H of 360 km·h^{-1} with a total electrical power consumption of 6961 W.

3.2. VTOL and Agility Characterizations

Figure 5 shows the tailsitter in stationary vertical hover using only the PTVC-M without the control surfaces. Electrical power consumption was 222 W per motor. The hovering was stable and all the rotational controls around the principal axes were found to be authoritative. As the PTVC-M did not require control surfaces to work, it enabled the aircraft to perform inverted vertical hover, as shown in **Figure 6**. This would represent a true "four-dimensional" (4D) aerobatic flyer. The aircraft could comfortably perform an inverted vertical climb at a rate of 5 ms^{-1} before the aerodynamic moments from the surfaces overwhelmed those generated by the PTVC-M. The major aerodynamic difference between the upright and inverted hovers is that the former involved propeller wash effects due to the presence of downstream surfaces (e.g. wings and stabilizers). Subsequent characterizations in this section referred to the upright case, since it is the more likely configuration to be used for VTOL.

The maximum rates of the control response at near zero airspeed were 180˚s^{-1}, 220˚s^{-1} and >700˚s^{-1} for the roll, pitch and yaw, respectively, but the effectiveness of PTVC-M dropped off with increasing airspeed. Strengthening of the PTVC-M yaw moment as the airspeed approached zero is similar to the fact that a multi-engine airplane with an engine failure will experience a larger yaw moment at low airspeed [28].

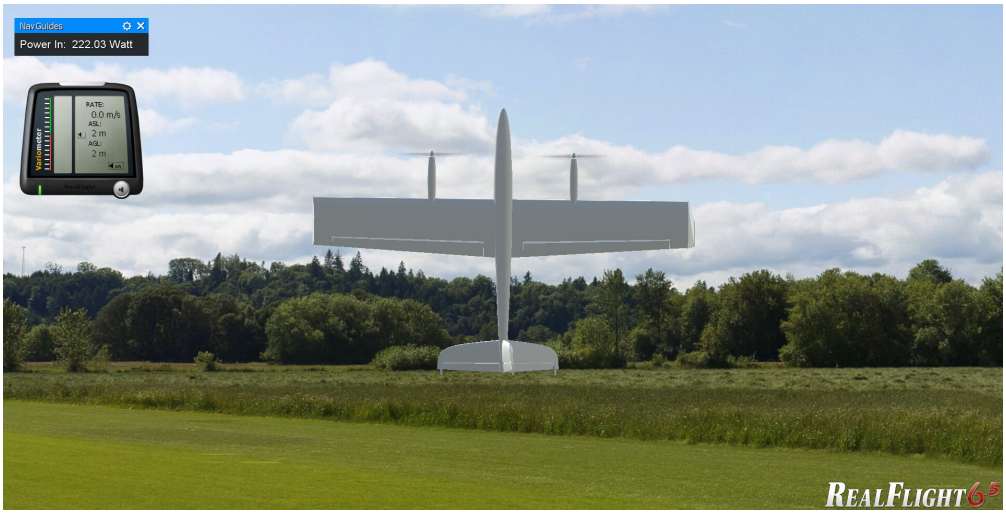

Figure 5. The tailsitter in a stationary hover using only the PTVC-M.

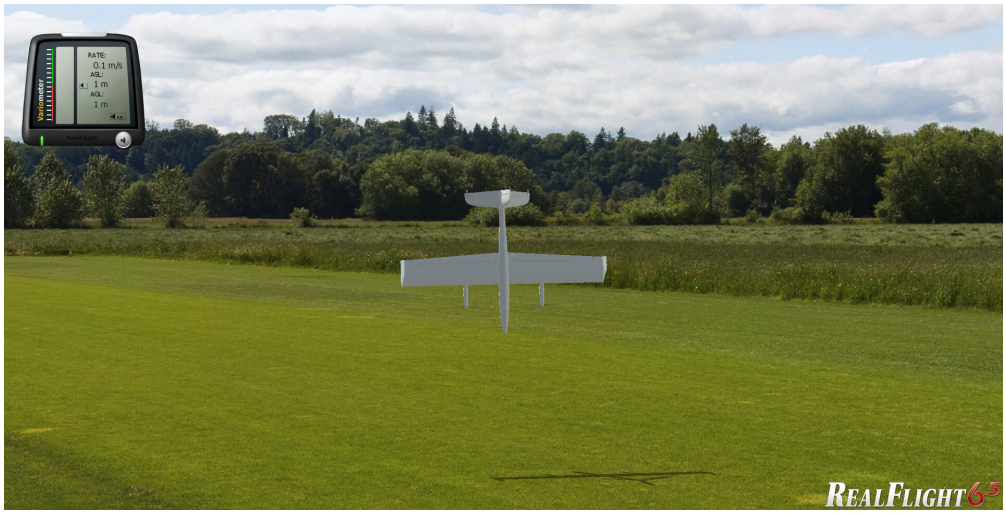

Figure 6. Inverted vertical hover made possible with the surface-free PTVC-M. Variometer shows a climb rate of 0.1 ms^{-1}.

A more comprehensive study on the control effectiveness of PTVC-M as a function of airspeed was carried out and the test method involved launching the tailsitter vertically on its own propeller thrusts. When the airspeed has reached the desired constant value, maximum input was applied to the roll. The test was evaluated at airspeeds of 60 and 150 km·h^{-1} and the process was repeated for the pitch and yaw (**Table 1**). While the roll rates can be regarded as equilibrium values, the rotational rates for the pitch and yaw were considered as quasi-state values before significant change in directional heading occurred which would alter the airspeed, and hence the rotational rates. The responsiveness of the control surfaces was evaluated using the same vertical launch procedure and they too were summarized in **Table 1**. Results indicated that the PTVC-M and the control surfaces are complementary, in that the control surfaces generally worked well at high speed, while the PTVC-M gave good response below 60 km·h^{-1}. This means that post-stall flights including VTOL could be primarily handled by the PTVC-M while the control surfaces could be optimized for other phases of flight thereby, eliminating the performance tradeoffs between VTOL and high speed cruise commonly encountered in VTOL airplane design.

The ailerons continued to work below the wing-stall speed of 39 km·h^{-1} because they were immersed in the strong propeller wash. The elevators managed to exert an angular rate of 50˚s^{-1} at zero airspeed due to the widening of the wake flow angle during the static hover (0 km·h^{-1} airspeed) [23]. As expected, the aerodynamic rudder control completely stalled at zero airspeed due to lack of propeller wash in its vicinity.

The rolls of the simulated tailsitter were quite axial and have low tendency to cause directional change or promote angular momentum exchange among the principal axes of the aircraft [23]. Thus, it was possible to acquire the equilibrium roll rates attributed to the PTVC-M and the control surfaces for airspeeds ranging from 0 to 190 km·h^{-1}, as shown in **Figure 7**. The aileron roll rate was 230˚s^{-1} at 0 km·h^{-1} and increased to 1215˚s^{-1} at 190 km·h^{-1}. The PTVC-M, on the other hand, gave a slow roll rate of only 14˚s^{-1} at 190 km·h^{-1}. Furthermore, **Figure 7** suggests that the VTOL roll control could be adequately handled using only ailerons since it has good roll rates in the post-stall region (0 to 39 km·h^{-1}).

Setting the throttle to maximum while the aircraft was in hovering position and applying full deflection of pitch control resulted in a pitch rate of no less than 650˚s^{-1}, which could be used to create a new form of maneuver based on the well-known “waterfall” maneuver [29]. This unique maneuver is available as a demonstration video (**Video 1**). The rapid yaw rate of the PTVC-M would benefit the development of high-performance spinsonde which will be covered in the next section of this article.

Video 2 shows the general VTOL and cruise flight performance of the tailsitter such as hovering, transition to forward flight (and vice versa), loop, and rolls. The maximum controlled vertical descent rate was found to be 8 ms^{-1}. The landing sequence from level flight to final touchdown could be performed with ease, an indication that the coupling between the control surfaces and the PTVC-M has resulted in responsive controls that seamlessly spanned across the full flight envelope.

3.3. Spinsonde Performance

Spinsonde is a concept developed to acquire high-resolution vertical wind speed profile measurements for atmospheric research [30]. It is a chute-free vertical retardation technique which enables multi-cycle measurements to be performed within a single flight and it is based on the stall-spin maneuver [30]. Multi-cycle measurement is not attainable with conventional expendable dropsondes [31]. This section explores the spinsonde capability of the aircraft whose primary flight controls involved the PTVC-M working in tandem with the aerodynamic surfaces.

Table 1. Comparison of angular rates about the principal axes due to PTVC-M and control surfaces at various airspeeds.

Control mode	Airspeed (km h^{-1})	Rotations about the principal axes (˚s^{-1})		
		Roll	Pitch	Yaw
PTVC-M	0	180	220	>700
	60	70	110	35
	150	24	80	25
Control surfaces	0	230	50	0
	60	497	180	115
	150	1030	330	140

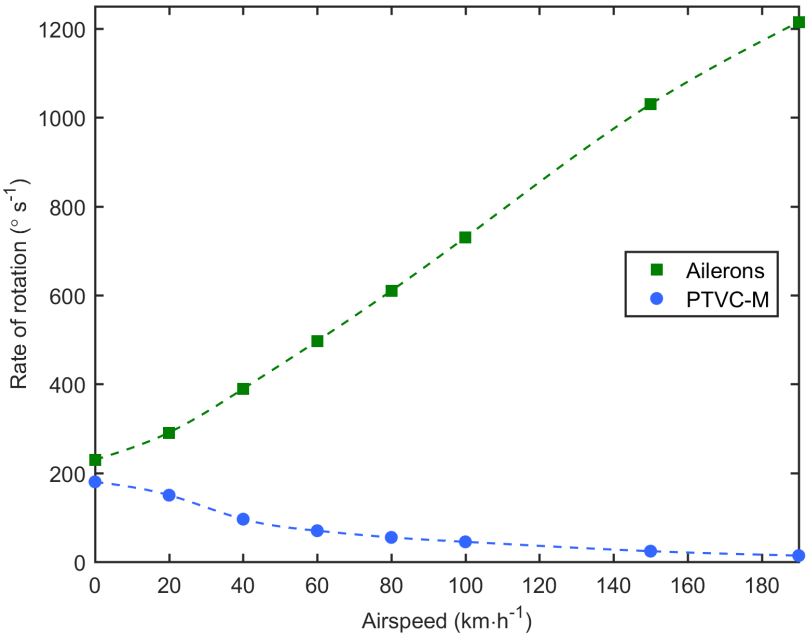

Figure 7. Equilibrium roll rates attributed to ailerons and PTVC-M as a function of airspeed.

The simulated tests were carried out for horizontal wind speeds of 0 km·h^{-1}and approximately 40 km·h^{-1} (altitude and terrain dependent) and the results for both scenarios are available in **Video 3**. The arrows in the second part of the video indicate the direction of wind flow. Also, the local wind intensity and updraft are displayed on the NavGuides. The steady-state stall-spin was generally achieved by applying maximum deflection of rudder and ailerons in the same direction and applying up elevator with no throttle input. For the 0 km·h^{-1} wind, it achieved an equilibrium descent rate of 6.2 ms^{-1}, and the variation between the wind speed and ground speed was ±3 km·h^{-1}, which was taken as the measurement uncertainty of the wind speed following [30]. The spinsonde performance was further characterized at wind intensity of around 190 km·h^{-1} as shown in **Figure 8**, and the spinsonde continued to work very well despite the uncertainty has slightly increased (with largest deviation being ±8 km·h^{-1}). The aircraft experienced orographic downdrafts because it has drifted behind the hills. The binocular gadget window provides a magnified view of the aircraft in real-time. Note that the ground speed would be equivalent to the speed measurement acquired by the onboard GPS if it were in real field testing [30].

In mesoscale meteorology, the parameter of particular interest to forecasters and the public is the maximum sustained 10-m surface wind [32], but so far it proved challenging to acquire such measurement using spinsonde technique without incurring risks to the safety of the aircraft [30]. **Video 3** shows that PTVC-M not only helped to provide vertical retardation to the spinsonde, but with some throttle input, the aircraft was able to climb while gyrating in the stall-spin. The maneuver was repeated under windy condition with success (**Video 3**). **Figure 9** is a screenshot of the aircraft performing a steady climb at the conclusion of a stall-spin at a height of just 3 meters above ground level with a climb rate of 3.5 ms^{-1}. In other words, the PTVC-M has given the aircraft the ability to climb in a powered stall-spin, serving as a mean to safely exit the maneuver at low altitude, thus making it possible to incorporate the 10-m surface wind into the multi-cycle measurement of vertical wind speed profile.

4. Conclusion

We had proposed and demonstrated via simulations the concept of PTVC-M in an attempt to develop ultra-agile VTOL capabilities without relying on large control surfaces which often degrade high-speed flight performance. The small UAV in this work equipped with PTVC-M had demonstrated the ability to perform inverted vertical hover with full 3-axis control. PTVC-M had also enabled the UAV to climb in a stall-spin and such feature will

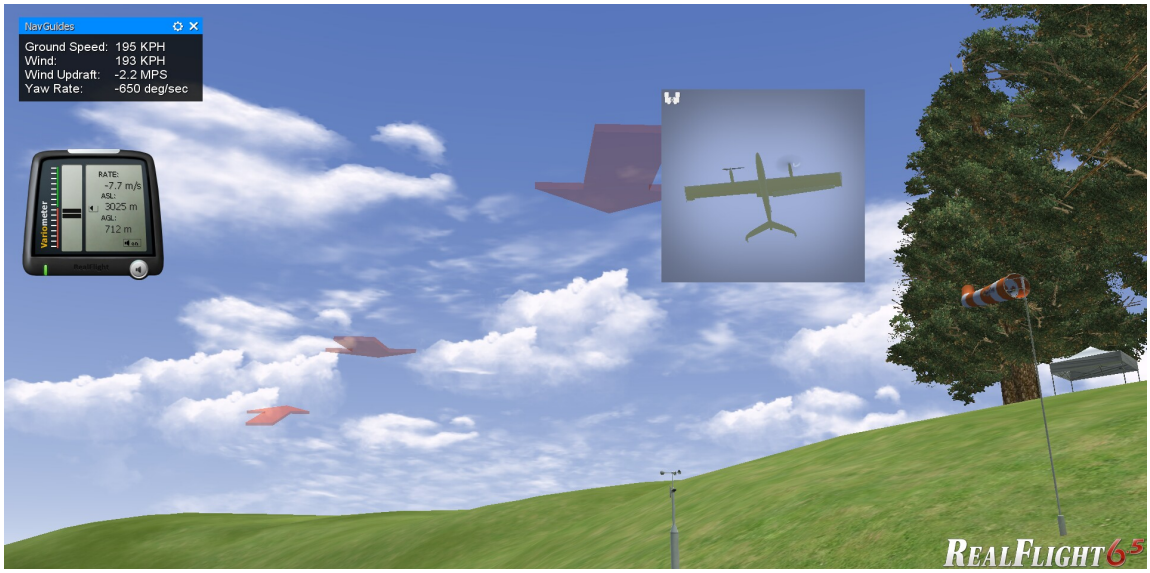

Figure 8. Evaluating the spinsonde performance in strong wind.

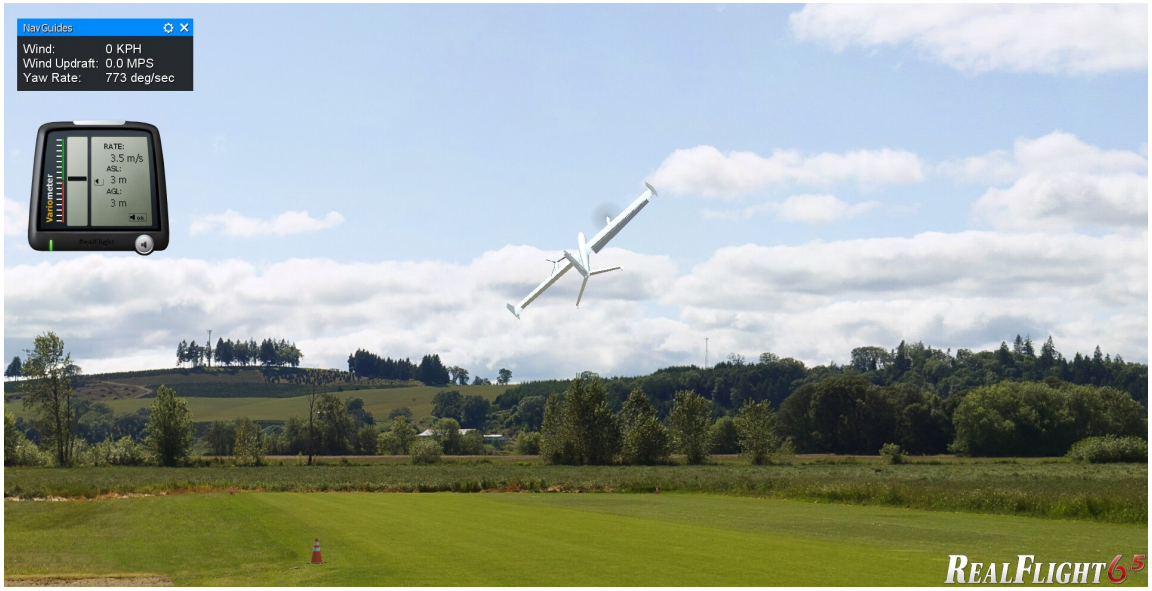

Figure 9. The aircraft performing a powered stall-spin with positive climb rate of 3.5 ms^{-1} at a height of 3 m above the ground. The direction of spin is anticlockwise (viewed from above).

lead to the development of high-performance spinsonde that can directly measure the 10-m surface wind intensity as part of the multi-cycle measurement of the vertical wind speed profile. We believe the proposed PTVC-M will be another indispensable tool in mesoscale meteorology as well as being an enabling technology that brings exciting and enthralling "4D" maneuvers to the world of sport aerobatics.

References

[1] Gyroplanepassion.com (2016) Inventor of the Autogiro. http://www.gyroplanepassion.com/Juan_de_la_Cierva.html

[2] Marchand, A. (2016) A Spanish Pioneer. http://www.airbushelicopters.com/w1/jrotor/71/delacierva.html

[3] Hitchens, F. (2015) The Encyclopedia of Aerodynamics. Andrews UK Limited, Bedfordshire.

[4] Sport Copter International (2016) About Gyroplanes. http://www.sportcopter.com/Gyroplanes/tabid/124/Default.aspx

[5] Century of Flight (2016) The History of Flight. http://www.century-of-flight.net/Aviation%20history/evolution%20of%20technology/VTOL%20and%20STOL%20Technology%20and%20Aircraft.htm

[6] Wikipedia (2016) Fairey Rotodyne. https://en.wikipedia.org/wiki/Fairey_Rotodyne

[7] Wikipedia (2016) Yakovlev Yak-141. https://en.wikipedia.org/wiki/Yakovlev_Yak-141

[8] Sanchez, A., Escareño, J., Garcia, O. and Lozano, R. (2008) Autonomous Hovering of a Noncyclic Tiltrotor UAV: Modeling, Control and Implementation. *Proceedings of the* 17*th World Congress of the International Federation of Automatic Control*, Seoul. http://dx.doi.org/10.3182/20080706-5-kr-1001.00138

[9] Poh, C.H. and Poh, C.K. (2014) Can the Vertical Motions in the Eyewall of Tropical Cyclones Support Persistent UAV Flight? *Journal of Aeronautics & Aerospace Engineering*, **3**, 133.

[10] Vargas-Clara, A. and Redkar, S. (2012) Dynamics and Control of a Stop Rotor Unmanned Aerial Vehicle. *International Journal of Electrical and Computer Engineering*, **2**, 597. http://iaesjournal.com/online/index.php/IJECE/article/view/1589 http://dx.doi.org/10.11591/ijece.v2i5.1589

[11] Australian Aviation (2013) Australian Company Designs New Stoprotor Aircraft Technology. http://australianaviation.com.au/2013/04/australian-company-designs-new-stoprotor-aircraft-technology/

[12] ELYTRON Aircraft Inc. (2013) Design. http://elytron.aero/#page-aircraft

[13] Latitude Engineering (2016) Hybrid Quadrotor™ Technology. https://latitudeengineering.com/products/hq/

[14] ComQuest Ventures LLC (2016) The Vertex VTOL UAS. http://www.comquestventures.com/vertex-vtol-uas/

[15] Selig, M.S. (2010) Modeling Full-Envelope Aerodynamics of Small Uavs in Real Time. *Proceedings of the AIAA Atmospheric Flight Mechanics Conference*, 7635.

[16] International Miniature Aerobatic Club (2009) About IMAC. http://www.mini-iac.com/

[17] The World Air Sports Federation (2016) F3M Large Radio Control Aerobatics World Cup. http://www.fai.org/world-cups/f3m

[18] SEBART International Srl (2016) Sebart 50E ARF Assembly Manual. http://www.sebart.it/download/manuale%20Sebart%2050/Manual%20introduction%20Sebart-50E.pdf

[19] Wikipedia (2016) Thrust Vectoring. https://en.wikipedia.org/wiki/Thrust_vectoring

[20] ArduPilot Development Team (2016) What Is a MultiCopter and How Does It Work? http://ardupilot.org/copter/docs/what-is-a-multicopter-and-how-does-it-work.html

[21] Leishman, J.G. (2000) Principles of Helicopter Aerodynamics. 2nd Edition, Cambridge University Press, New York.

[22] Armattan Quads (2016) Tricopters. http://www.armattanquads.com/tricopters/

[23] Selig, M.S. (2010) Modeling Propeller Aerodynamics and Slipstream Effects on Small UAVs in Realtime. *Proceedings of the AIAA Atmospheric Flight Mechanics Conference*, Toronto, 2-5 August 2010, 7938. http://dx.doi.org/10.2514/6.2010-7938

[24] Autodesk Inc. (2016) 3ds Max® 3D Modeling, Animation, and Rendering Software. http://www.autodesk.com/products/3ds-max/overview

[25] Great Planes® Model Mfg. (2015) RealFlight® Radio Control Flight Simulator. http://www.realflight.com/

[26] Knife Edge Software (2014) KEmax Content Creation Toolkit. http://www.knifeedge.com/KEmax/

[27] Hepperle, M. (2004) MH 22. http://www.mh-aerotools.de/airfoils/mh22koo.htm

[28] Commercial Aviation Safety Team (2016) Asymmetric Flight. http://www.cast-safety.org/pdf/5_asymmetric_flight.pdf

[29] YouTube (2016) Waterfall. https://www.youtube.com/watch?v=feuyIIVRR2w

[30] Poh, C.-K. and Poh, C.-H. (2015) Concept of Spinsonde for Multi-Cycle Measurement of Vertical Wind Profile of Tropical Cyclones. *Open Journal of Applied Sciences*, **5**, 145-150. http://dx.doi.org/10.4236/ojapps.2015.54015

[31] Wikipedia (2016) Dropsonde. http://en.wikipedia.org/wiki/Dropsonde

[32] Franklin, J.L., Black, M.L. and Valde, K. (2003) GPS Dropwindsonde Wind Profiles in Hurricanes and Their Operational Implications. *Weather and Forecasting*, **18**, 32-44. http://dx.doi.org/10.1175/1520-0434(2003)018<0032:GDWPIH>2.0.CO;2